Monthly Notices
of the
ROYAL ASTRONOMICAL SOCIETY

MNRAS **457,** 267–271 (2016) doi:10.1093/mnras/stv2964

Circumgalactic medium of quasars: C IV absorption systems

M. Landoni,[1]★ R. Falomo,[2] A. Treves,[3] R. Scarpa[4] and E. P. Farina[5]

[1]*INAF, Osservatorio Astronomico di Brera, via E. Bianchi 46, Merate (LC), Italy*
[2]*INAF, Osservatorio Astronomico di Padova, vicolo dell'Osservatorio 5, Padova (PD), Italy*
[3]*Universita' degli Studi dell'Insubria, via Valleggio 11, Como (CO), Italy*
[4]*Instituto de Astrofisica de Canarias (IAC), C/ Via Láctea, s/n, E-38205 La Laguna, Tenerife, Spain*
[5]*Max-Planck-Institut für Astronomie, Königstuhl 17, D-69117 Heidelberg, Germany*

Accepted 2015 December 16. Received 2015 December 16; in original form 2015 November 6

ABSTRACT

We investigate the properties of circumgalactic gas in the halo of quasar (QSO) host galaxies from C IV absorption-line systems. We use the optical spectroscopy of closely aligned pairs of quasars (projected distance ≤ 200 kpc) obtained at the Gran Telescopio Canarias to investigate the distribution of the absorbing gas for a sample of 18 quasars at $z \sim 2$. We have found that the detected absorption systems of EW ≥ 0.3 Å associated with the foreground QSOs are revealed up to 200 kpc from the centre of the host galaxy. The structure of the absorbing gas is patchy with a covering fraction of the gas that quickly decreases beyond 100 kpc. These results are in qualitative agreement with those found for the lower ionization metal Mg II λ2800 Å.

Key words: quasars: absorption lines – quasars: general.

1 INTRODUCTION

Direct observation of low-redshift galaxies ($z \leq 1$) has demonstrated the presence of large and diffuse warm-to-hot gas haloes up to ~ 200 kpc, commonly referred to as the circumgalactic medium (CGM); see, for example, Lanzetta et al. (1995), Chen et al. (2001) and Churchill, Steidel & Kacprzak (2005). In the last decades, a number of papers have exploited absorption lines imprinted in the spectra of background quasars (QSOs) to investigate the physical properties of the CGM (e.g. Bahcall & Spitzer 1969; Churchill et al. 2005; Nielsen et al. 2013a; Nielsen, Churchill & Kacprzak 2013b), finding significant correlation between the absorptions of the gas in the CGM and the global properties of galaxies, such as luminosity (Chen & Tinker 2008), mass (Churchill et al. 2013), colour (Zibetti et al. 2007) and star formation rate (Prochter, Prochaska & Burles 2006; Ménard et al. 2011; Nestor et al. 2011). Nevertheless, only a few studies have been focused on the properties of the gaseous halo of galaxies hosting a QSO in their centre (see Hennawi et al. 2006; Hennawi & Prochaska 2007, and references therein).

The standard model for the origin of the extreme luminosity of QSOs considers that a supermassive black hole shines when intense mass inflow takes place, possibly as a consequence of tidal forces in dissipative events (Di Matteo, Springel & Hernquist 2005). In this scenario, the CGM of QSOs is expected to be populated by tidal debris, streams and cool gas clouds, as commonly observed in interacting galaxies (e.g. Sulentic et al. 2001; Cortese et al. 2006). Moreover, the gas of the CGM belonging to the QSO host galaxy could be metal-enriched by supernova-driven winds triggered by starbursts events associated with the mergers or by QSO-driven outflows of gas (e.g. Steidel et al. 2010; Shen & Ménard 2012). Although in the last few years a great effort has allowed us to detect emission lines that arise from the CGM (Hennawi & Prochaska 2013; Martin et al. 2014; Cantalupo et al. 2014; Hennawi et al. 2015), only the Lyman α feature has been observed so far. For these reasons, the most efficient way to study the CGM is to investigate the absorption features that it imprints in the spectra of background QSOs (e.g. Adelberger et al. 2005; Hennawi et al. 2006).

In this context, projected QSO pairs are ideal observational tools for this purpose, because the light of the very bright source in the background ($z = z_{\rm B}$) goes through the extended halo of the foreground ($z_{\rm F} < z_{\rm B}$) object (e.g. Hennawi et al. 2006; Farina et al. 2013). The absorption features in the gaseous haloes belonging to the foreground QSO can therefore be exploited to understand the processes of enrichment of material far from the host galaxy. In this paper, we aim to characterize the properties of intervening C IV absorbers in the CGM of QSO host galaxies up to a projected distance (PD) of 200 kpc. We adopt the following cosmological parameters: $H_0 = 70\,{\rm km\,s^{-1}\,Mpc^{-1}}$, $\Omega_{\rm m} = 0.27$ and $\Omega_\Lambda = 0.73$.

2 SAMPLE SELECTION

In order to investigate the properties and abundances of C IV in the CGM of QSOs, we selected QSO projected pairs by searching the Sloan Digital Sky Survey Data Release 10 of spectroscopic quasars (Pâris et al. 2012). We assume as good candidates pairs those with PD (comoving transverse distance) smaller than 200 kpc in order to characterize the innermost region of the CGM. Further, we constrain the line-of-sight (LOS) velocity difference, based on the published

★ E-mail: marco.landoni@brera.inaf.it

Table 1. Properties of the observed pairs: pair identification (ID); position of the foreground target (RA, Dec.); foreground redshift (z_F); background redshift (z_B); V apparent magnitudes of foreground and background QSO (V_F, V_B); projected distance in kpc (PD); signal-to-noise ratios (per pixel) of foreground and background object (SN_F, SN_B).

ID	RA_F	$Dec._F$	z_F	z_B	V_F	V_B	PD	SN_F	SN_B
QQ01	08:45:13.57	+39:10:25.65	2.040	2.210	19.8	19.5	180	15	15
QQ02	09:17:06.47	+00:56:35.10	2.140	2.472	20.4	20.2	200	10	10
QQ03	10:13:01.20	+40:23:03.52	2.185	2.504	18.4	19.2	192	35	20
QQ04	12:06:51.22	+02:04:21.90	2.443	2.522	20.5	19.0	110	15	20
QQ05	13:58:06.09	+61:18:26.70	2.015	2.167	20.5	20.2	190	10	15
QQ06	14:30:33.61	–01:34:45.69	2.273	2.350	19.5	19.5	55	10	10
QQ07	09:13:23.31	+04:02:35.15	2.040	2.375	19.1	19.5	92	15	15
QQ08	09:16:11.20	–01:19:41.50	2.753	2.917	20.7	20.8	87	15	10
QQ09	10:09:35.86	+47:49:34.61	2.292	2.590	20.7	19.7	93	5	15
QQ10	11:34:26.18	+00:38:54.86	2.209	2.365	20.4	19.6	90	15	20
QQ11	00:42:52.23	+01:11:55.62	2.027	2.084	18.7	18.9	70	30	30
QQ12	03:44:11.98	+00:09:27.88	2.125	2.240	21.4	19.4	184	10	25
QQ13	12:14:31.06	+32:23:28.24	1.978	2.271	19.5	20.0	202	10	10
QQ14	08:45:33.63	+25:15:51.64	2.110	2.292	19.0	20.3	186	15	5
QQ15	12:19:30.15	+15:10:28.44	1.943	2.313	19.2	19.7	110	35	25
QQ16	12:21:49.62	+37:00:13.82	2.119	2.322	20.4	20.7	97	10	10
QQ17	14:59:06.93	+12:34:49.54	2.109	2.500	18.6	20.6	42	50	20
QQ18	15:53:19.30	+31:52:40.39	2.817	3.194	22.3	20.0	200	15	25

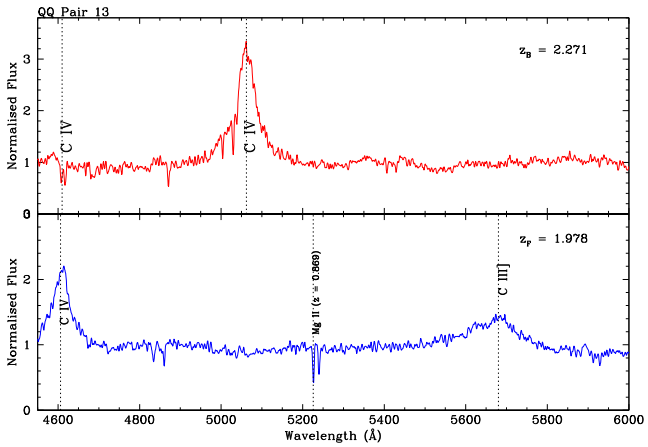

Figure 1. Normalized spectra of the pair QQ 13. The solid blue line is the spectrum of the foreground QSO while the red solid line is used for the background one. The most prominent quasar emission lines are also marked. In the spectrum of the foreground, we also detect an intervening Mg II absorption system at $z = 0.869$. The whole figure set is available in the online version of this paper as Supporting Information.

redshift, $\Delta V \geq 5000\,\mathrm{km\,s^{-1}}$, to ensure that pairs are not gravitationally bound. We also put a threshold on the magnitude of the background QSO ($m_r \leq 20$) to secure spectra with adequate signal-to-noise ratio ($\geq$15) and on declination to ensure good visibility from the Roque de los Muchachos observatory. Finally, we selected pairs in which the redshifts of the foreground and background QSOs combine, so that the C IV absorption lines at the redshift of the foreground (z_F) fall within the wavelength range 4500–6000 Å. This procedure yielded 34 candidate pairs. We selected 25 objects for observation, according to the visibility of the considered period. However, only 18 targets were obtained because of partially bad weather conditions. Details on the observed objects are reported in Table 1.

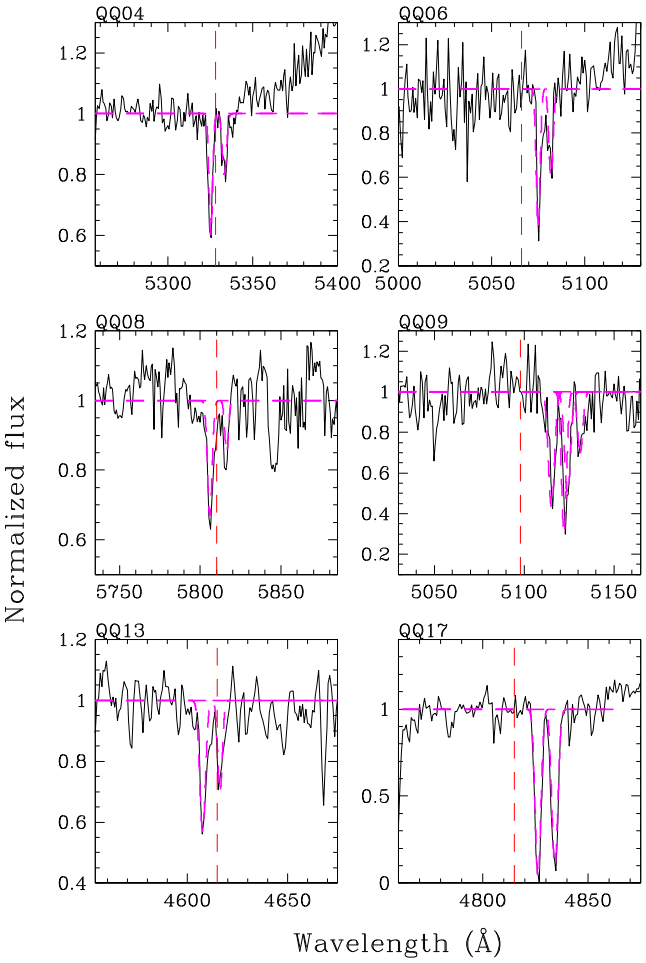

Figure 2. Normalized spectra of background quasars showing the intervening absorption feature identified as C IV 1548 Å and C IV 1550 Å that are close in velocity and projected distance from the foreground quasar (see text). The vertical dashed red lines indicate the positions of the C IV 1548 emission line in the spectrum of the foreground QSO.

Table 2. Measurement of the C IV absorption in the background QSO of each pair. the columns give the identification label (ID), C IV 1548–1551λ observed wavelength and equivalent widths (rest), doublet ratio (DR), velocity difference between the absorption redshift and the foreground QSO redshift, ΔV (km s^{-1}), EW minimum detectable on the spectrum (Å).

ID	λ_{abs}(1548) (Å)	W (1548) (Å)	λ_{abs}(1551) (Å)	W (1551) (Å)	DR	ΔV (km s^{-1})	EW$_{min}$ (Å)
QQ01B	–	–	–	–	–	–	0.13
QQ02B	–	–	–	–	–	–	0.12
QQ03B	–	–	–	–	–	–	0.10
QQ04B	5324	0.70 ± 0.20	5334	0.30 ± 0.10	2.30	–300	0.15
QQ05B	–	–	–	–	–	–	0.20
QQ06B	5075	1.30 ± 0.40	5084	0.60 ± 0.20	2.17	500	0.15
QQ07B	–	–	–	–	–	–	0.20
QQ08B	5805	0.50 ± 0.20	5817	0.30 ± 0.10	1.67	–500	0.25
QQ09B	5114	0.60 ± 0.20	5124	0.30 ± 0.10	2.00	600	0.18
QQ10B	–	–	–	–	–	–	0.20
QQ11B	–	–	–	–	–	–	0.16
QQ12B	–	–	–	–	–	–	0.10
QQ13B	4607	0.50 ± 0.20	4616	0.40 ± 0.15	1.25	–400	0.23
QQ14B	–	–	–	–	–	–	0.40
QQ15B	–	–	–	–	–	–	0.20
QQ16B	–	–	–	–	–	–	0.20
QQ17B	4824	0.50 ±0.10	4834	0.30 ± 0.05	1.67	600	0.20
QQ18B	–	–	–	–	–	–	0.18

3 OBSERVATIONS, DATA REDUCTION AND DATA ANALYSIS

We observed our QSO pairs with the 10.4-m Gran Telescopio Canarias (GTC) equipped with the Optical System for Imaging and Low Resolution Integrated Spectroscopy (OSIRIS; Cepa et al. 2003) from 2013 September to 2014 August. Observations were gathered with GTC–OSIRIS adopting the grism R2500V with a slit of 1.00 arcsec, yielding a resolution $\lambda/(\Delta\lambda) \sim 2500$ (1 px = 0.80 Å, corresponding to 45 km s^{-1} at the centre wavelength). In this case, the resolution corresponds to a FWHM of about 2 Å, allowing us to fully resolve the components of the C IV doublets (λλ1548–1551 Å). The resolution element, which corresponds to a FWHM of 120 km s^{-1}, is not sufficient to kinematically resolve the internal dynamics of the absorbing gas, which is beyond the aim of our investigation. For each pair, we oriented the slit in order to acquire simultaneously the spectra of the two objects and we secured three different exposures, applying a small shift of 5 arcsec along the slit to better reject cosmic rays and to account for CCD defects.

We reduced our data by the adoption of standard IRAF[1] procedures. Briefly, for each frame, we performed bias subtraction and flat-field correction using the CCDRED package. Wavelength calibration has been assessed through the observation of arc lamps (Xe+Ne+HgAr) and the residuals on the calibration are around 0.04 Å. We flux calibrated the spectra exploiting standard stars observed during the same nights of the targets. We corrected for systematics, slit losses and variation of the sky conditions through aperture photometry of the field, in the r' band, acquired shortly before the observation. We report an example of spectra of a pair in Fig. 1 and we give the full figure set in the online version of this paper. The Galactic reddening was taken into account considering the estimates from Schlegel, Finkbeiner & Davis (1998) assuming $R_V = 3.1$ (Cardelli, Clayton & Mathis 1989). In the spectra of the QSO presented in Fig. 1, in addition to the typical broad emission lines of C IV and C III, we note that several absorption lines due to intervening matter (e.g. Mg II at $z = 0.869$) are present. The C IV absorption system ascribed to the halo of the foreground QSO is also detected in some cases in the spectrum of the background QSO.

We performed the search of the C IV (λλ1548–1550) absorption doublet in the spectrum of the background QSO for each pair in an interval of wavelengths corresponding to 4000 km s^{-1} centred at the expected position of C IV lines at the redshift of the foreground QSO. In the case of detection, we fit the components by the adoption of two Gaussian profiles, as illustrated in the panels of Fig. 2. Furthermore, in order to properly characterize the quality of the data, in each window we measured the minimum detectable equivalent width (EW$_{min}$) by following procedure described in Sbarufatti et al. (2006). Briefly, we evaluated the EW on bins of the size of the resolution element in various regions of the spectrum excluding telluric structures. We assume as EW$_{min}$ the 2σ deviation from the mean of the average of the distribution of the EWs obtained in each bin. Finally, concerning the LOS velocities of the detected C IV absorptions, we considered that the system is associated with the foreground object only if $|\Delta V| \leq 500$–600 km s^{-1} rest frame. The results of our procedures are reported in Table 2.

4 RESULTS AND DISCUSSION

In six out of 18 pairs, we detected a C IV absorption system associated with the foreground QSO halo (see Table 2 and Fig. 2). In one case (QQ09), we have a suggestion of a double C IV system probably associated with two or more moving clouds belonging to the foreground QSO haloes. In this case, we deblended the features by fitting the four components adopting Gaussian profiles (see panel 4 of Fig. 2). We also note that in QQ10 a C IV absorption is detected at $\lambda \sim 4800$ Å in the spectrum of background QSOs, but we do not include it in our statistic because the velocity difference is slightly beyond our threshold. The EW of the detected associated

[1] IRAF is distributed by the National Optical Astronomy Observatories, which are operated by the Association of Universities for Research in Astronomy, Inc., under cooperative agreement with the National Science Foundation.

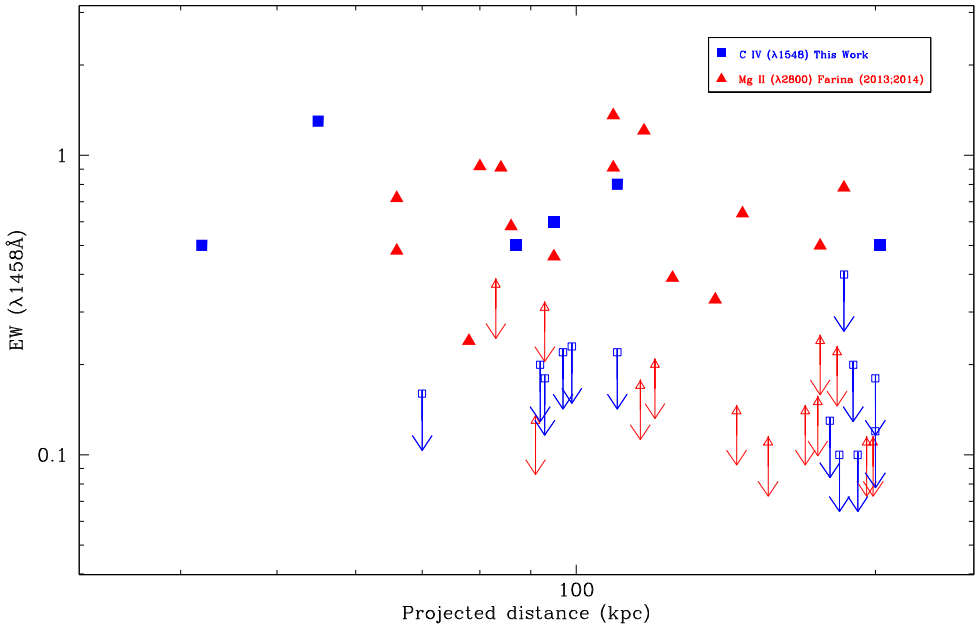

Figure 3. Equivalent width of C IV (filled blue squares) intervening absorption lines as a function of the projected distance from the quasar (including the upper limit of QQ10 from Farina et al. 2013). Upper limits are indicated by open squares with arrows (see text). Similar data are shown for Mg II 2800 absorption systems (filled red triangles) and their relative upper limits (open triangles with arrows) (Farina et al. 2013, 2014).

C IV absorption systems, together with the upper limits, are shown in Fig. 3 as a function of the projected separation from the foreground QSO. In spite of the relatively small statistics, considering both the detections and the upper limits, there is an indication that the absorbing systems decrease in intensity as a function of the distance from the centre of the (foreground) QSOs and that the absorbing gas becomes more patchy. We performed a Cox proportional hazard test including the uppers limits (Isobe, Feigelson & Nelson 1986) and found that the two quantities (PD and EW) are anticorrelated with a probability of ∼93 per cent. This behaviour is qualitatively very similar (see Fig. 3) to that of Mg II λ2800 Å intervening systems (Farina et al. 2013, 2014), although the average redshift of the objects is different ($\langle z \rangle = 1.2$ for Mg II compared with $\langle z \rangle = 2.1$ for C IV).

In order to quantify the patchy structure of the absorbing gaseous haloes, we investigate the covering fraction of (f_c) of C IV as a function of PD. We choose a threshold equivalent width $\mathrm{EW_{th}} = 0.30$ Å, which allows us to consider spectra with $\mathrm{EW_{min}} \leq 0.25$ Å, except for one case (QQ14), and two bins of [0–100] kpc and [100–200] kpc. For each bin, we define f_c as the ratio between detected systems over the total number of pairs in the bin. Because the analysis of the covering fraction is sensitive to the binning effect and depends on the adopted $\mathrm{EW_{th}}$, we combine our results, adopting the same EW_{th} for consistency with those recently drawn in the sample of Prochaska, Lau & Hennawi (2014); this yields seven extra sources. We find that the covering fraction for C IV is f_c ($\geq$0.30 Å) $= 0.63^{+0.10}_{-0.12}$ for the bin [0–100] kpc while for the bin [100–200] kpc, it is f_c ($\geq$0.30 Å) $= 0.25^{+0.10}_{-0.08}$ (see Fig. 4). The horizontal bars are the bin width while the vertical bars are the 1σ uncertainties in f_c calculated upon the binomial statistics (68 per cent Wilson score). We note that the f_c of C IV decreases by about a factor of 2 between the first bin (0–100 kpc) and the second bin (100–200 kpc). It is of interest to compare these results with those derived from the covering fraction of Mg II. Assuming the same bins and $\mathrm{EW_{th}}$, we computed f_c for Mg II by adopting data presented in Farina et al. (2013, 2014) for

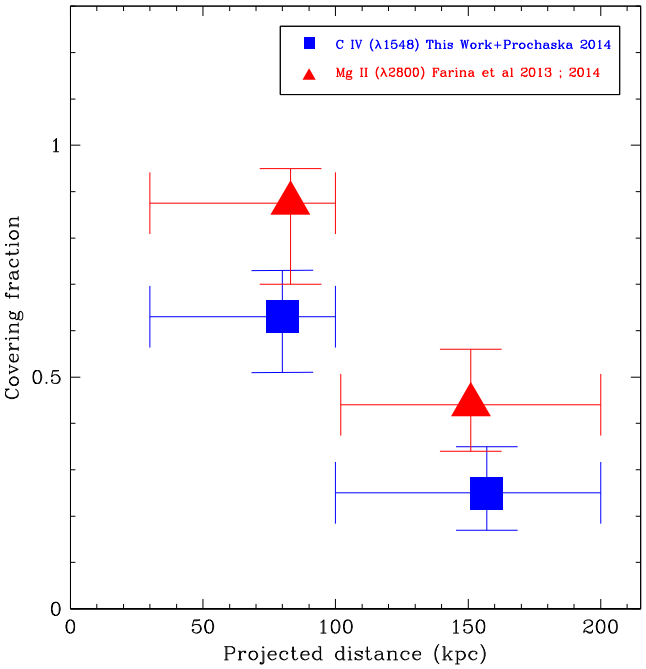

Figure 4. Covering fraction of C IV in QSO host galaxies (filled blue squares) derived from the combined sample (this work plus the data set by Prochaska et al. 2014; see text). For comparison, we report the covering fraction of Mg II derived from the data set considered in Farina et al. (2013, 2014) (see text). Vertical error bars are 1σ confidence level at 68 per cent Wilson score for a binomial distribution.

26 pairs. We found that f_c ($\geq$0.30 Å) $= 0.86^{+0.10}_{-0.09}$ for the bin [0–100] kpc and f_c ($\geq$0.30 Å) $= 0.45^{+0.13}_{-0.10}$ for the bin [100–200] kpc (see Fig. 4).

For both Mg II and C IV species, the covering fraction of the absorbing material is halved from the region (<100 kpc) close to

the centre of the host galaxy to the immediate outer region (100–200 kpc). There is a suggestion that the covering fraction of C IV absorbers is systematically smaller than that of Mg II. This behaviour could be related, because of the different ionization energies of the two species and/or because of chemical abundances. We note that, although the statistics is small, our finding is also consistent with results based on C II and C IV for a sample of 60 QSO pairs (Prochaska et al. 2014).

ACKNOWLEDGEMENTS

EPF acknowledges funding through the ERC grant 'Cosmic Dawn'.

REFERENCES

Adelberger K. L., Shapley A. E., Steidel C. C., Pettini M., Erb D. K., Reddy N. A., 2005, ApJ, 629, 636
Bahcall J. N., Spitzer L. Jr, 1969, ApJ, 156, L63
Cantalupo S., Arrigoni-Battaia F., Prochaska J. X., Hennawi J. F., Madau P., 2014, Nat, 506, 63
Cardelli J. A., Clayton G. C., Mathis J. S., 1989, ApJ, 345, 245
Cepa J. et al., 2003, Proc. SPIE, 4841, 1739
Chen H-W., Tinker J. L., 2008, ApJ, 687, 745
Chen H-W., Lanzetta K. M., Webb J. K., Barcons X., 2001, ApJ, 559, 654
Churchill C., Steidel C., Kacprzak G., 2005, Extra-Planar Gas, 331, 387
Churchill C. W., Nielsen N. M., Kacprzak G. G., Trujillo-Gomez S., 2013, ApJ, 763, L42
Cortese L., Gavazzi G., Boselli A., Franzetti P., Kennicutt R. C., O'Neil K., Sakai S., 2006, A&A, 453, 847
Di Matteo T., Springel V., Hernquist L., 2005, Nat, 433, 604
Farina E. P., Falomo R., Decarli R., Treves A., Kotilainen J. K., 2013, MNRAS, 429, 1267
Farina E. P., Falomo R., Scarpa R., Decarli R., Treves A., Kotilainen J. K., 2014, MNRAS, 441, 886
Hennawi J. F., Prochaska J. X., 2007, ApJ, 655, 735
Hennawi J. F., Prochaska J. X., 2013, ApJ, 766, 58
Hennawi J. F. et al., 2006, ApJ, 651, 61
Hennawi J. F., Prochaska J. X., Cantalupo S., Arrigoni-Battaia F., 2015, Sci, 348, 779
Isobe T., Feigelson E. D., Nelson P. I., 1986, ApJ, 306, 490
Lanzetta K. M., Bowen D. V., Tytler D., Webb J. K., 1995, ApJ, 442, 538
Martin D. C., Chang D., Matuszewski M., Morrissey P., Rahman S., Moore A., Steidel C. C., 2014, ApJ, 786, 106
Ménard B., Wild V., Nestor D., Quider A., Zibetti S., Rao S., Turnshek D., 2011, MNRAS, 417, 801
Nestor D. B., Johnson B. D., Wild V., Ménard B., Turnshek D. A., Rao S., Pettini M., 2011, MNRAS, 412, 1559
Nielsen N. M., Churchill C. W., Kacprzak G. G., Murphy M. T., 2013a, ApJ, 776, 114
Nielsen N. M., Churchill C. W., Kacprzak G. G., 2013b, ApJ, 776, 115
Pâris I. et al., 2012, A&A, 548, A66
Prochaska J. X., Lau M. W., Hennawi J. F., 2014, ApJ, 796, 140
Prochter G. E., Prochaska J. X., Burles S. M., 2006, ApJ, 639, 766
Sbarufatti B., Treves A., Falomo R., Heidt J., Kotilainen J., Scarpa R., 2006, AJ, 132, 1
Schlegel D. J., Finkbeiner D. P., Davis M., 1998, ApJ, 500, 525
Shen Y., Ménard B., 2012, ApJ, 748, 131
Steidel C. C., Erb D. K., Shapley A. E., Pettini M., Reddy N., Bogosavljevic M., Rudie G. C., Rakic O., 2010, ApJ, 717, 289
Sulentic J. W., Rosado M., Dultzin-Hacyan D., Verdes-Montenegro L., Trinchieri G., Xu C., Pietsch W., 2001, AJ, 122, 2993
Zibetti S., Ménard B., Nestor D. B., Quider A. M., Rao S. M., Turnshek D. A., 2007, ApJ, 658, 161

SUPPORTING INFORMATION

Additional Supporting Information may be found in the online version of this article:

Suppl-Online-Material.pdf
(http://www.mnras.oxfordjournals.org/lookup/suppl/doi:10.1093/mnras/stv2964/-/DC1).

Please note: Oxford University Press is not responsible for the content or functionality of any supporting materials supplied by the authors. Any queries (other than missing material) should be directed to the corresponding author for the article.

This paper has been typeset from a TEX/LATEX file prepared by the author.